ORGANIC PROCESS RESEARCH & DEVELOPMENT
OPR&D

pubs.acs.org/OPRD Article

Process Development of a Second Generation β-Amyloid-Cleaving Enzyme Inhibitor—Improving the Robustness of a Halogen-Metal Exchange Using Continuous Stirred-Tank Reactors

Bryan Li,* Richard W. Barnhart, Amelie Dion, Steven Guinness, Alan Happe, Cheryl M. Hayward, Jeffrey Kohrt, Teresa Makowski, Mark Maloney, Jade D. Nelson, Asaad Nematalla, J. Christopher McWilliams, Zhihui Peng, Jeffrey Raggon, John Sagal, Gerald A. Weisenburger, Denghui Bao, Miguel Gonzalez, Jiangping Lu, Mark D. McLaws, Jian Tao, and Baolin Wu

Cite This: *Org. Process Res. Dev.* 2021, 25, 1440−1453 Read Online

ACCESS | Metrics & More | Article Recommendations

ABSTRACT: Process development for the synthesis of a second generation β-amyloid-cleaving enzyme (BACE1) inhibitor (**1**) is described. The lithiothiazole addition to the isoxazolene (**5**) under batch conditions was not scalable because of reaction gelling and anion instability. A continuous stirred-tank reactor flow process was developed and successfully executed on the 70 kg scale in multiple runs. In a head-to-head comparison between the continuous and batch processes, the former was clearly superior as it gave a higher yield (80 vs 63%) of the adduct (**4**) and better reaction control for handling the unstable lithiothiazole as a reaction intermediate. Subsequently, **4** underwent Pd-catalyzed amination with *t*-butyl carbamate, reductive cleavage of the N−O bond, thioamidine cyclization, and deprotection of the Boc group to provide hydropyranothiazine **2**. The synthesis of **1** was completed by amidation with 5-(difluoromethoxy)picolinic acid and the successive deprotection of the benzamide group with either Silicycle-diamine or L-lysine.

KEYWORDS: *BACE1, halogen-metal exchange, CSTR, continuous process, lithiothiazole*

1. INTRODUCTION

β-site amyloid precursor protein-cleaving enzyme 1 (BACE1) is involved in the production of the β-amyloid (Aβ) peptide, a neurotoxin which is believed to play a key role in the development of Alzheimer's disease.[1] Reducing levels of Aβ by inhibition of BACE1 have been vigorously pursued as a therapeutic strategy to improve cognitive function in Alzheimer's models.[2] Among these candidates, thiazinamines have shown potential as selective BACE1 inhibitors with improved potency and reduced side effects and are the subject of ongoing clinical development.[3] Recent endeavors from the Pfizer research team led to the discovery of a potent, selective BACE1 inhibitor (**1**, Scheme 1)[3b] targeting Alzheimer's disease. The compound displayed good safety, tolerability, and pharmacokinetics from phase I clinical trials.[4] As BACE1 was an ongoing drug-discovery program, our exploratory active pharmaceutical ingredient support strategy was to develop convergent synthesis such that it would accommodate structural modifications of each of the substructures of the thiazinamine series (A, B, and C, Scheme 1) from SAR studies without compromising the delivery timelines.

2. RESULTS AND DISCUSSION

2.1. Thiazole Anion Addition to Isoxazolene 5. To support the continuous development of the thiazinamine series of clinical candidates, our efforts were focused on enabling a similar route[3b] by the Discovery chemistry team for scale up.[5] In this route[3b] (Scheme 2), 2,4-dibromothiazole (**6**) underwent lithium-halogen exchange regioselectively at the C-2 position under cryogenic conditions. The rigid isoxazolene (**5**) ring structure allowed a high degree of stereocontrol leading to thiazole anion addition to the convex face, proving **4** as the sole product. Nevertheless, there were multiple complications in scaling this reaction:

1 Gelling of the reaction mixture. On gram scale reaction in the laboratory, the solution of **5** in toluene/THF (10:1 ratio) was added to the reaction mixture containing lithiothiazole **7** as fast as possible. Within minutes of the addition, gelling occurred causing the stirring to stop. It was found that the reaction gelling would not occur if the reaction mixture was maintained at −90 °C during the addition of isoxazolene (**5**). While this approach effectively resolved the gelling issue, the reaction yield was modest at 57% yield after chromatographic isolation. Furthermore, batch size was limited to

Received: April 12, 2021
Published: May 24, 2021

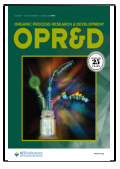

https://doi.org/10.1021/acs.oprd.1c00126
Org. Process Res. Dev. 2021, 25, 1440−1453

Scheme 1. Retrosynthesis of 1

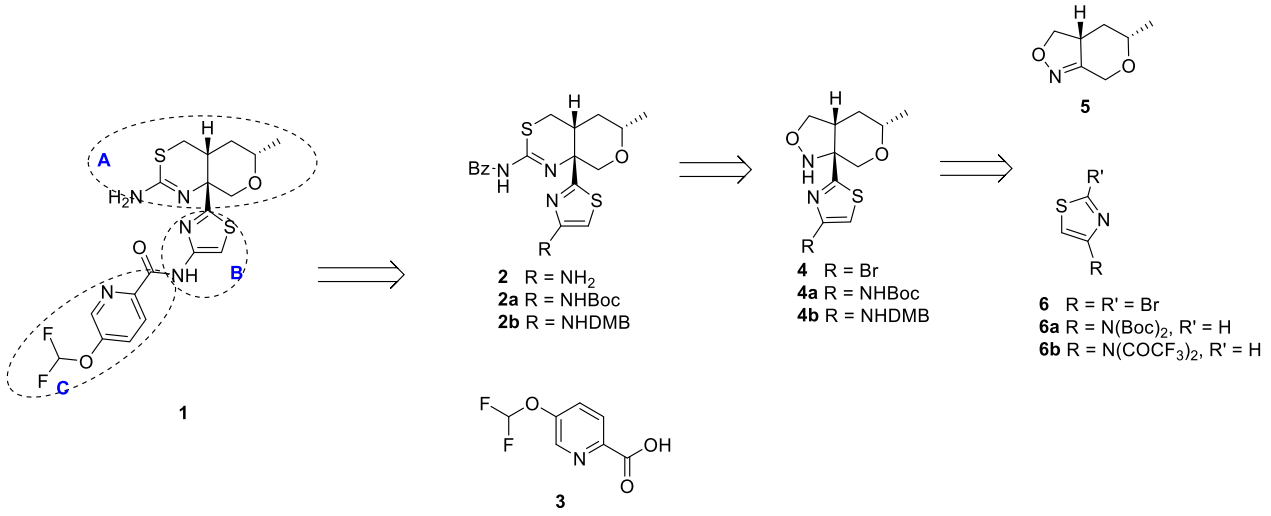

Scheme 2. Lithiation of 2,4-Dibromothiazole and Synthesis of 4

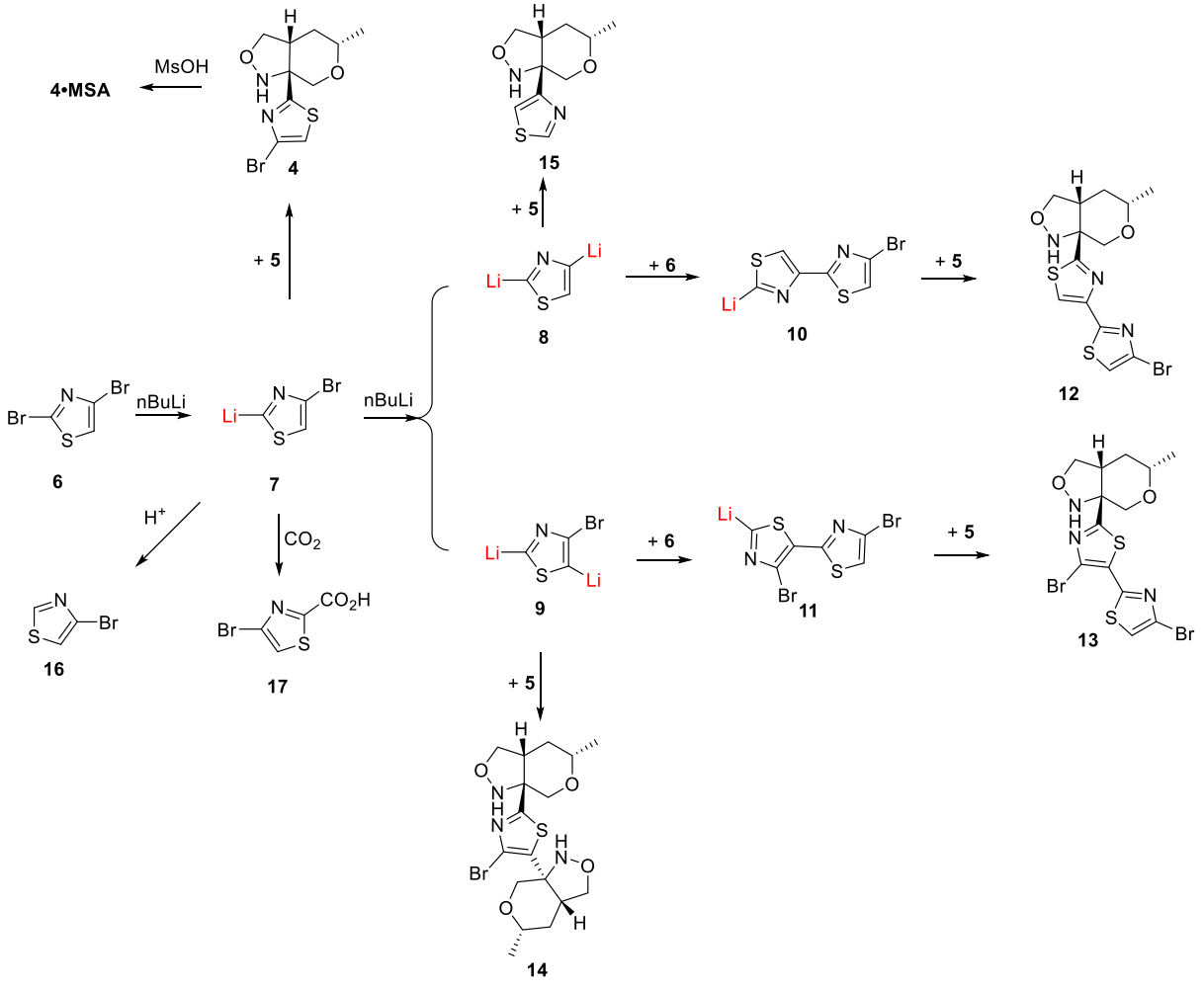

~9 kg in a 500 L reactor due to the stringent requirement for heat exchange.

2 Anion stability issue. During the lithium-bromo exchange, *n*-BuLi was slowly added to a suspension of 2,4-dibromothiazole (**6**) in a solvent under cryogenic conditions.[6] The extremely exothermic Li−Br exchange reaction, coupled with the poor solubility of **6** in all aprotic solvent systems studied, made it a challenge for scale up. Lithiothiazole **7** was capable of undergoing further lithiation to give dilithiated species **8** and **9**, which further reacted with **6** to generate monolithiated species **10** and **11**, respectively, giving rise to impurities

https://doi.org/10.1021/acs.oprd.1c00126
Org. Process Res. Dev. 2021, 25, 1440−1453

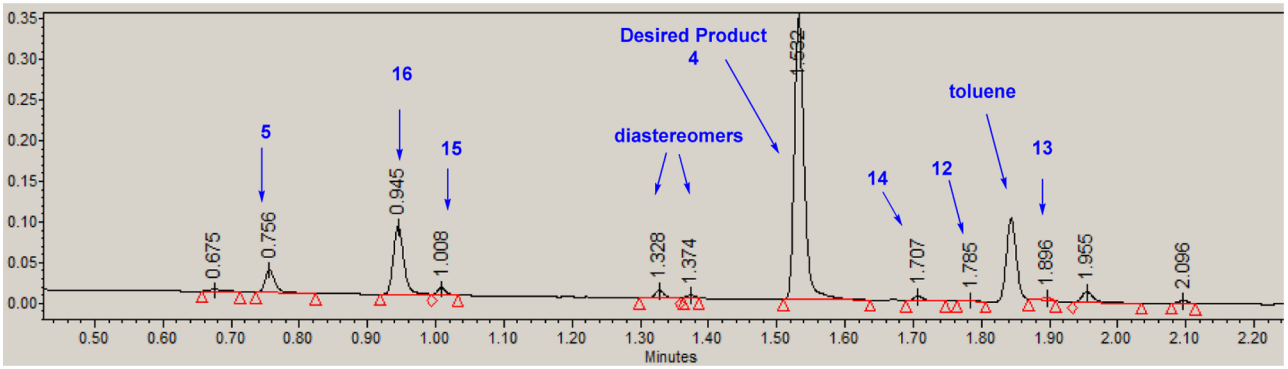

Figure 1. UPLC reaction profile of lithiothiazole addition to isoxazolene **5**.

12 and **13**. The formation of **14** was also observed from the reaction of dilithiothiazole **9** with **5**. A des-bromo impurity **15** was also noted, albeit at a relatively low level, presumably from the addition of **8** to **5**. A typical chromatogram of the reaction under very careful control of all operational steps is shown in Figure 1. When the reaction was carried out above the 10 g scale, the UPLC reaction profile started to become messy because the reaction time was prolonged to accommodate both stages of *n*-BuLi and isoxazolene addition. Elevating the reaction temperature above cryogenic conditions was known to be detrimental giving higher levels of both isomeric and other impurities.

3 Chromatographic isolation of the product **4**. While pure **4** was a crystalline solid, direct crystallization of the product from the reaction mixture was elusive. This was attributed to a modest crude product purity of ~80% or lower, which impeded the crystallization; it could not be facilitated by seeding. Under the circumstance, silica gel chromatography was utilized for product isolation. A major byproduct as shown in Figure 1 was bromothiazole **16**, generated from excess lithiothiazole **7** after reaction quench. In early attempts, carbon dioxide was used to quench the reaction, followed by aqueous quench, which converted **7** to its corresponding carboxylic acid **17**, providing a purging handle for aqueous extraction. However, it introduced operational complexity for further scale up.

As the project quickly moved through the development pipeline, we were tasked to develop a scalable process under an expedited timeline. It was clear that the anion addition step was a bottleneck for the overall synthesis, and we started to tackle multiple challenges (*vide supra*) simultaneously.

2.1.1. Selection of Solvents. The solubility of dibromothiazole **6** in all solvents was rather poor at cryogenic temperatures. As the reaction appeared to perform best in a THF/toluene mixture, we focused on the volumetric ratio of these solvents for the reaction. A quick survey showed that the gelling issue was closely related to the volumetric ratio of toluene and THF. When the toluene/THF ratio was 10:1 and total volume was ~40 vol, a serious gelling problem was observed. At the same total solvent volume, gelling was no longer observed at −75 °C or lower temperature when the solvent ratio of 2:1 (v/v) was employed (Table 1). While the cause for gelling is not fully understood, it appears to be related to complexation of isoxazolene **5** with BF_3·OEt_2. THF complexes with BF_3 competitively, hence breaking up the gelling. It is noteworthy

Table 1. Study of the Impact of the Toluene/THF Ratio on Reaction Fluidity

		u1		
entry	ratio toluene/THF	reaction time (min)	conversion of **5** (%)	comments
1	2:1	60	97	fluid below −75 °C
2	4:1	60	97	gelling at −69 °C
3	10:1	60	97	gelling at −55 to −65 °C

that THF also acts as a coordinating solvent to enhance the reactivity by dissociating *n*-BuLi hexamers in hexane to form more reactive tetramers and dimers.[7] Conversely, the significantly increased amount of THF has a deleterious effect on the reaction kinetics, and this necessitated a super-stoichiometric amount of BF_3·OEt_2. Overall, the use of THF as a cosolvent was a good trade-off by allowing the reaction to be operable on scale by eliminating the gelling concern.

2.1.2. Methanesulfonic Acid Salt Formation of 4. In parallel to the reaction development, efforts were directed to streamline the workup and isolation. As the calculated pK_a of **4** is 3.28 (in water), there was a reasonable hope to find a suitable salt of the product to facilitate product isolation. A salt screen led to discovery of a highly crystalline methanesulfonic acid salt of **4** (**4**·MSA). A solvent screen identified acetonitrile as being ideal for crystallization, which allowed direct isolation of 97.7% pure product from the ~80% pure crude mixture (Table 2). Further enhancement of the purity of **4** could be accomplished with a salt break from methanol and aqueous NaOH. High recovery of the free base **4** could be achieved by recrystallization from methanol. With this process, laboratory scale up afforded crystalline product **4** as a free base in 77.4% isolated yield with 99.2% purity. It is noteworthy that 4-bromothiazole (**16**), which would interfere in the downstream reaction, was completely rejected. In this improved product isolation protocol, carbon dioxide quenching was no longer required and a simple aqueous NH_4Cl solution quench was used instead to enable more convenient scale up.

2.1.3. Adapting the Process to Continuous Flow. The highly exothermic nature of the Li−Br exchange dictates the slow combination of *n*-BuLi and **6** to control the reaction temperature.[10] The adiabatic temperature rise could be as high as 61.9 °C under a worst-case scenario.[8] Since the surface-to-volume ratio decreases substantially as the reaction is scaled up in a batch reactor, a dramatic decrease in heat exchange capacity results. The poor solubility of dibromooxazole **6** in the reaction solvent(s) further complicated the matter. On an early

https://doi.org/10.1021/acs.oprd.1c00126
Org. Process Res. Dev. 2021, 25, 1440−1453

Table 2. Workup with Methanesulfonic Acid Salt Formation for 4

materials		UPLC profile (area %) 5	16	4	yield	product loss
crude product before salt formation		2.4%	11.6%	79.1%	83.6%	
salt formation with MSA in MeCN	MSA salt	0.1%	0.4%	97.7%	81.8%	
	mother liquor	10.7%	46.6%	10.1%		2.1%
salt break in MeOH	product	0.1%	ND	99.2%	77.4%[a]	
	mother liquor	3.0%	10.2%	49.0%		3.1%

[a]Overall yield from the reaction, salt formation, and salt break.

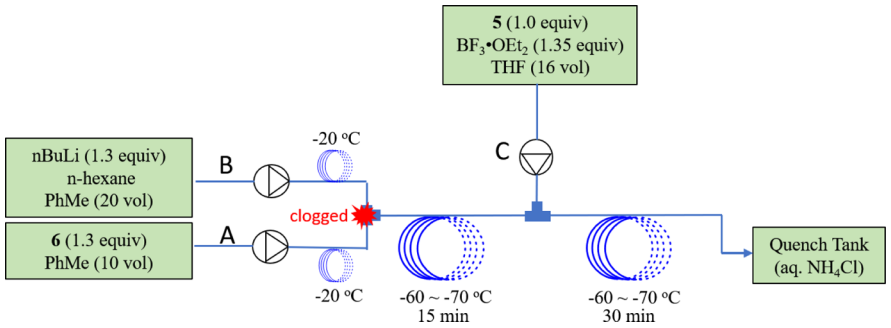

Figure 2. PFR schematic diagram for the continuous flow process.

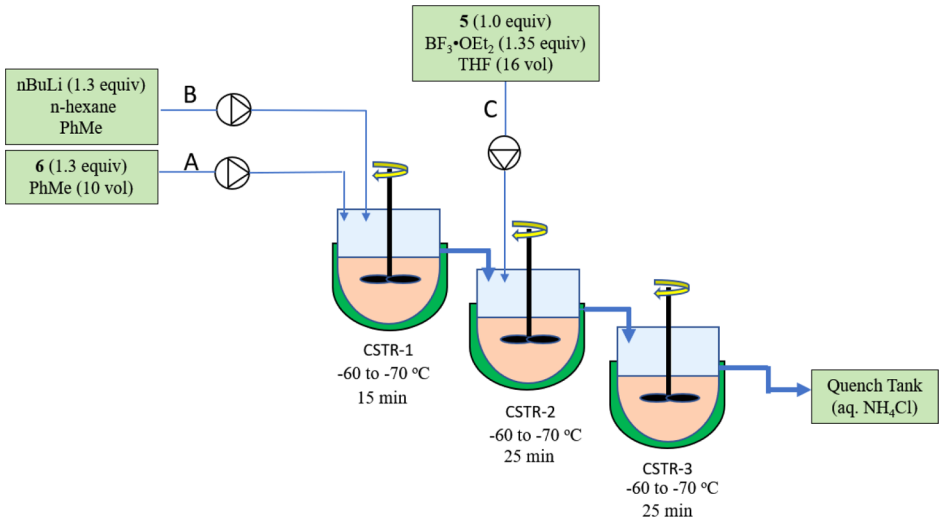

Figure 3. Laboratory CSTR design for the continuous process.

9.0 kg scale batch reaction in a 500 L reactor, the addition time was 12.7 h. As discussed earlier, prolonged Li−Br exchange time is detrimental to the reaction due to the formation of impurities **12**, **13**, **14**, and **15**. Since the anion stability and the long duration of the Li−Br exchange reaction were major concerns, it became evident that continuous flow technology could be more optimal for this reaction. Continuous processes offer many advantages over batch methods, including precise control of stoichiometry, reaction time and temperature, high reproducibility, and often better reaction yields.[9] The much higher surface area-to-volume ratio under flow conditions allows highly efficient heat transfer. When coupled with a much smaller volume in the reaction train, safety hazards in handling exothermic reactions are minimized. This is particularly attractive as the stability of lithiothiazole **7** is a major concern in this process. Thus, subsequent development of this critical transformation was directed toward enablement of a continuous option. Both plug-flow reactor (PFR) and continuous stirred-tank reactor (CSTR) approaches were considered. A PFR approach was first tested.[10] The solution of **6** in toluene at RT was pumped into a coil and mixed with *n*-BuLi solution in hexane/toluene via a T-mixer. The lithiation was designed to take place in the first coil and the resulting anion would react with **5** in a second coil. Both coils were set in a cooling bath between −60 and −70 °C (Figure 2), and precooling of each feed stream was carried out to address the high exothermicity. Unfortunately, tube clogging at the T-mixer was observed due to precipitation of **6** at this low temperature. The clogging issue was mainly due to the significantly decreased solubility of **6**,[11] and this appeared as an insurmountable problem under PFR conditions.

CSTR arrangements are more able to handle heterogeneous mixtures, so we redirected our laboratory assessment (Figure 3). Thus, the solution of **6** in toluene at RT and the solution of *n*-BuLi (in hexane, diluted with toluene) were independently pumped (precooled at −20 to −30 °C before mixing at CSTR)

https://doi.org/10.1021/acs.oprd.1c00126
Org. Process Res. Dev. 2021, 25, 1440−1453

Table 3. Flow Parameter Study of the CSTR Process at −60 to −70 °C[a]

	conditions				IPC (area %)			
			residence time					
entry	toluene/THF volume ratio	total volume (vol)	lithiation (min)	anion addition (min)	**5**	**16**	**4**	*in situ* yield[b]
1	2:1	45	15	25 × 2	3.0%	12.8%	77.6%	82.4%
2	2:1	45	8	15 × 2	2.4%	10.7%	81.4%	85.4%
3	2:1	30	11	20 × 2	2.8%	10.9%	80.9%	84.9%
4	2:1	30	6	10 × 2	2.4%	11.6%	79.1%	83.6%

[a]20 g of **5** was used for each experiment. [b]Potency adjusted yield by UPLC area %.

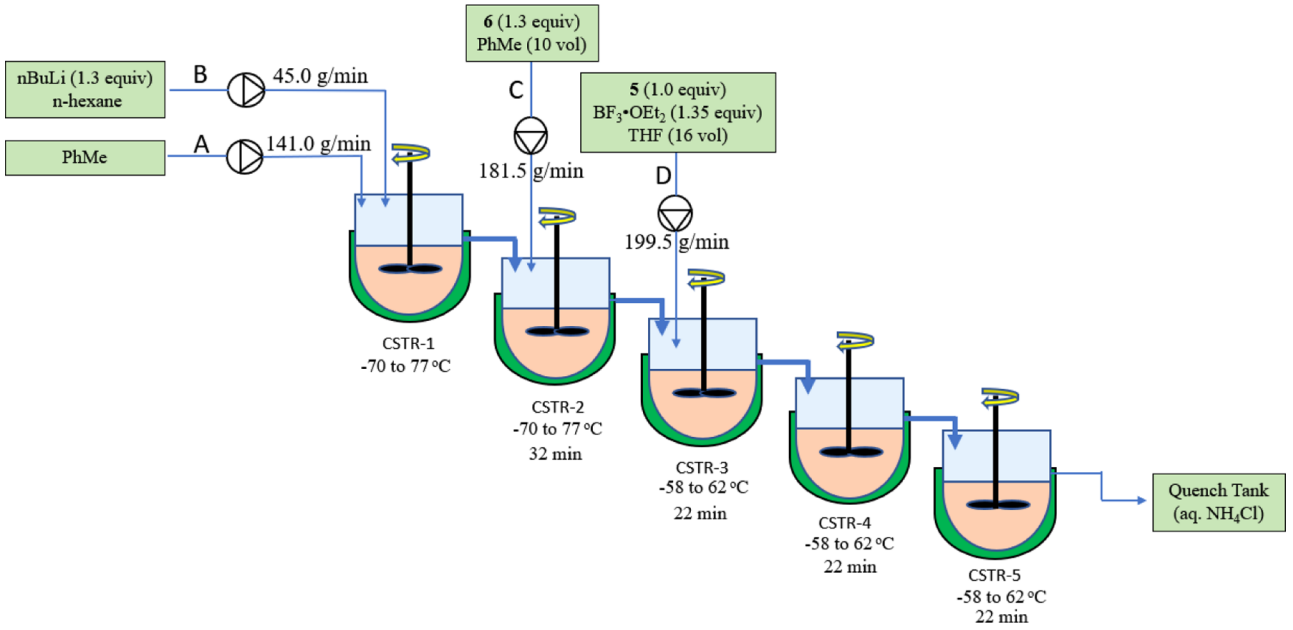

Figure 4. CSTR (5 × 13 L) for continuous process scale up.

into and mixed in the first CSTR for 15 min at −60 to −70 °C. The *in situ*-generated anion solution overflowed by gravity into a second CSTR, which contained a solution of **5** premixed with $BF_3{\cdot}OEt_2$ in THF that was continuously charged. The combined reaction mixture stayed in the second and third CSTR at −60 to −70 °C for 25 min each (τ, average residence time of volume/flow rate) each, before the reaction was quenched by aqueous NH_4Cl solution in the reservoir tank. In a representative laboratory CSTR run (Figure 3), the collected reaction mixture indicated ∼97% conversion of **5** to **4** in 82.4% *in situ* yield. It was notable that the contents in CSTR1 through CSTR3 did not appear fully homogeneous but remained highly fluid.[12] The gravity overflow between reactors enabled mass transfer obviating any need for a mechanical pumping mechanism. At the designed flow rates, passage time for the reaction mixture through the well-insulated transfer lines (1/4″ ID) was on the order of seconds, and clogging was not observed.

Using the same CSTR setup, the impact of residence time and solvent volume was investigated (Table 3). The toluene/THF ratio was kept at 2:1 to maintain fluidity of the reaction mixture, but the total reaction solvent was reduced from 45 to 30 vol successfully. Residence times for both lithiation (6−15 min) and anion addition (20−50 min) stages were found to have a good degree of flexibility, which enabled a wide process window for scale up reactor design. With the CSTR process, **12**, **13**, **14**, and **15** were no longer observed as major impurities, which was attributed to the shorter lithiation time compared to batch conditions.

2.1.4. CSTR Design for Production. We next moved to scale up the continuous process and selected 5 × 20 L jacketed stainless-steel CSTRs installed in series, as shown in Figures 4 and 5. The CSTRs were designed with two exit outlets allowing adjustment of the maximum residence volume at either 13 or 20 L. To reduce safety concerns with handling *n*-BuLi, the first CSTR was used to prepare and precool (−75 to −85 °C) a solution of *n*-BuLi in toluene. Lithiation was designed to occur in the second CSTR, with the last three

Figure 5. In-series CSTR used in the continuous process.

https://doi.org/10.1021/acs.oprd.1c00126
Org. Process Res. Dev. 2021, 25, 1440−1453

Table 4. Comparison of Process Parameters of the Previous and Updated Process

process		previous batch mode	batch mode with improved conditions	flow mode with improved conditions
scale		9.0 kg	24 kg	70 kg (2×) & 43 kg
reactor size (L)		500 L	1500 L	13 L × 5 CSTR
lithiation	Solvents	toluene/THF (2:1)	toluene/THF (4.4:1)	toluene/THF (2:1)
	Temperature	−70 to −77 °C	−94 to −87 °C	−70 to −77 °C
	reaction time	14.8 h	12.7 h	32 min
anion addition	Solvents	toluene/THF (2:1)	toluene/THF (4.4:1)	toluene/THF (2:1)
	Temperature	−58 to −62 °C	−92 to −97 °C	−58 to −62 °C
	reaction time	2.1 h	9.7 h	65 min
work up/isolation		CO_2 quench SiO_2 chromatography recrystallization with EtOAc/heptane	aq NH_4Cl quench MSA formation recrystallization with MeOH/NaOH (aq)	aq NH_4Cl quench MSA formation recrystallization with MeOH/NaOH (aq)
isolated yield		57%	63%	78−80%
product purity		96%	99%	99%

Scheme 3. Synthesis of Hydropyranothiazine 2[a]

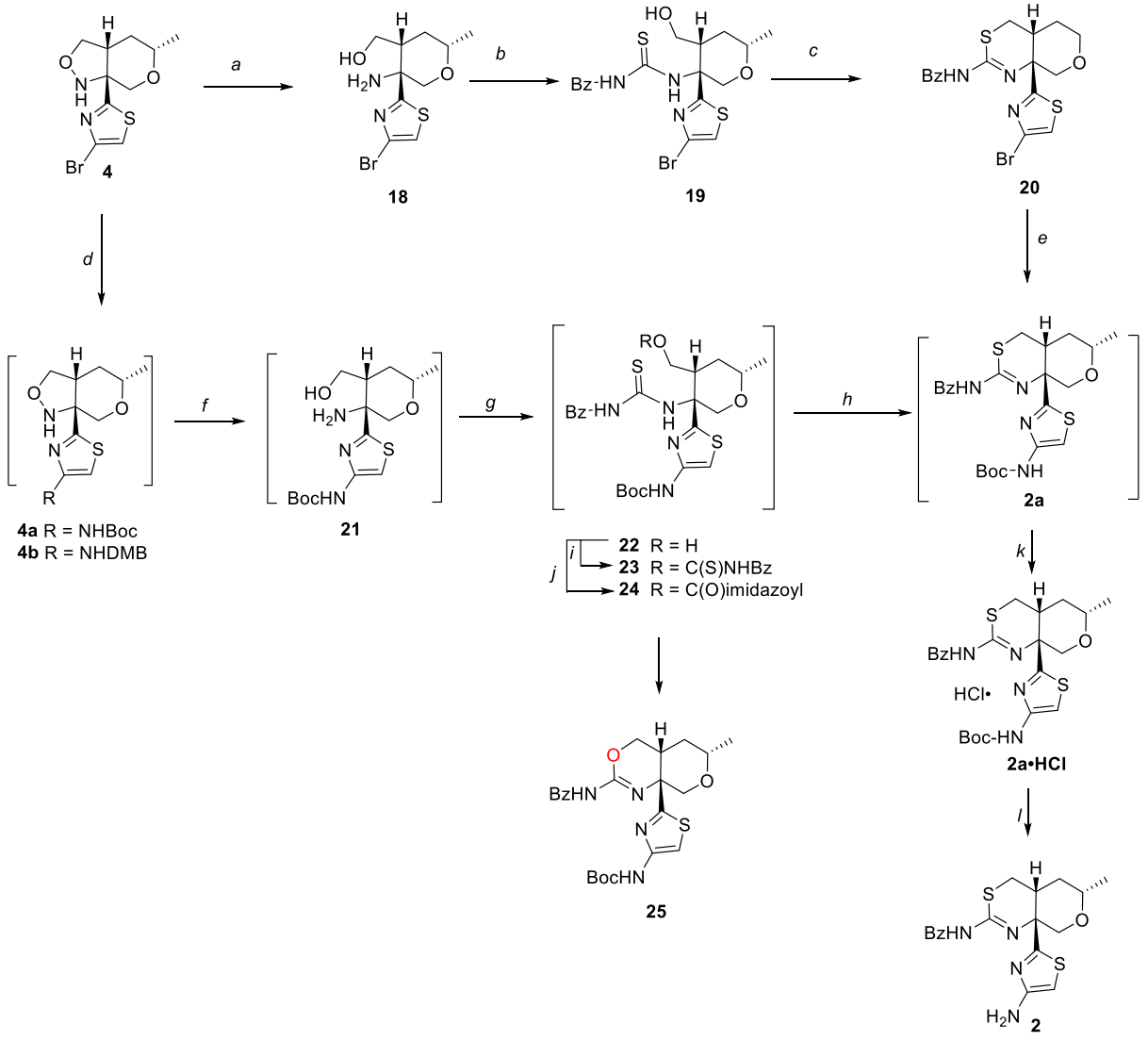

[a]Reagents and conditions: (a) $Mo(CO)_6$, CH_3CN, H_2O, $NaBH_4$, 70 °C, 95%; (b) benzoyl isothiocyanate, DCM, rt, 66%; (c) Ghosez's reagent, DCM, rt, 77%; (d) $BocNH_2$, $Pd_2(dba)_3$, tBuXPhos and K_2CO_3, toluene, reflux. 80−85% *in situ*; (e) $BocNH_2$, $Pd_2(dba)_3$, tBuXPhos and K_2CO_3, toluene, reflux. 78%; (f) Raney-Ni, H_2, 2-PrOH, 25 to 35 °C, 69% overall 2 steps d and f; (g) benzoyl isothiocyanate, THF, 50 °C, not isolated; (h) 48 to 60 °C, not isolated; (i) benzoyl isothiocyanate, THF, 50 °C, not isolated; (j) CDI, THF, 50 °C, not isolated; (k) aq HCl, EtOAc. RT, 82% overall 4 steps g, j, h and k; (l) concn HCl, then quenched to TEA/EtOAc, 70%.

https://doi.org/10.1021/acs.oprd.1c00126
Org. Process Res. Dev. 2021, 25, 1440−1453

CSTRs dedicated to anion addition. Material transfer between CSTRs was enabled by gravity via insulated stainless-steel transfer lines (1/4″ ID). Finally, the product stream was directed to a 5000 L glass-lined reactor containing an aqueous NH_4Cl solution for reverse batch quenching and isolation. Special attention was paid to the heat exchange requirements as the Li−Br exchange reaction is a fast and extremely exothermic reaction (*vide supra*). Due to limitations of the available cooling media (−70 °C at its lowest temperature) and the limited cooling capacity available within the plant, flow rates were decreased to maintain the continuous lithiation temperature and subsequent anion addition at −55 to −65 °C. The residence time for lithiation and anion addition was increased to 32 and 65 min, respectively, compared to 15 and 50 min employed in laboratory pilots. Fortunately, the reaction conversion and impurity profile were not affected by the longer reaction time (Tables 3 vs 4). This may be explicated by the fact that processing duration of the lithiation in the CSTR mode was only ∼3% of that in the batch mode (Table 4). Three batches with 43−70 kg input were completed using this CSTR process, providing product in 78.1−80.3% isolated yield with 99% purity (Table 4).

In this campaign, we also ran a head-to-head comparison between the continuous process and the batch process incorporating all improvements. Thus, a 24 kg scale was carried out under batch conditions using a 1500 L stainless-steel reactor. The isolated yield was ∼15% lower than that of the flow process. It was noticed that in batch, there was significantly more tar-like material formed that may be attributed to the much longer lithiation time (888 min vs 32 min). In addition, the flow process also provided other benefits such as reduced equipment size (Table 4), reduced safety risk (much smaller amount of *n*-BuLi in the reactor train), and reduced failure risk, that is, allowing reaction control by timely adjustment of the flow rate or pausing the feed as needed; therefore, the entire batch of starting materials was not committed should there be an unforeseen equipment or reaction failure.

2.2. Synthesis of Hydropyranothiazine 2. In the original synthesis,[3b] the preparation of **2** proceeded with a reductive cleavage of the N−O bond to give amino alcohol **18**, followed by the formation of thioamidine **19** and ring closure to give **20** (Scheme 3). To keep the C-3 bromo group on the thiazole intact, N−O bond cleavage was accomplished using $Mo(CO)_6$ and $NaBH_4$. The removal of Mo-related byproducts and the addition of $NaBH_4$ proved challenging when scaled to tens of grams. The addition of $NaBH_4$ required careful control as it was accompanied by hydrogen gas evolution and a large exotherm. Since this was clearly not ideal for scale up, we reordered the synthetic steps by moving the amination step upfront (Scheme 3), therefore circumventing the need of chemoselective reduction of the hydroxylamine in the presence of the thiazoyl bromide.

2.2.1. C−N Cross Coupling. The amination of **4** worked well using dimethoxybenzylamine (DMB-NH_2) to give **4b** (Scheme 3). However, deprotection of the DMB group in the downstream step resulted in moderate purity of the product and modest yield despite the use of chromatography for product isolation. Considering the convenience of Boc deprotection, *t*-butyl carbamate ($BocNH_2$) was selected as the coupling partner. After briefly screening both Pd- and Cu-mediated coupling reactions with $BocNH_2$, a set of conditions employing $Pd_2(dba)_3$, ^{t}BuXPhos, and K_2CO_3 in toluene were identified. The reaction provided **4a** in 80−85% *in situ* yield, but chromatography was required to isolate the product. Thus, we chose to telescope the crude product into the next step for scalability purpose and avoid yield loss.

2.2.2. N−O Reductive Cleavage. Raney-Ni-catalyzed hydrogenolysis was found optimal and it offered quantitative conversion to amino alcohol **21**. Isopropanol was found to be a good solvent for the reaction, while use of methanol gave rise to an N-methylated impurity. The crude product **4a** could be telescoped directly into the Raney-Ni hydrogenolysis. The amino alcohol **21**, with a calculated pK_a of 6.1, offered an opportunity to remove the organic soluble ligands and impurities (from the upstream Pd-coupling reaction) with an acid−base aqueous extractive workup.[13] Isolation of **21** was accomplished with good yield and high purity by crystallization from toluene. However, we found it more convenient and efficient to carry the crude product forward as a solution to the immediate downstream step, where purity upgrade opportunities were more apparent (*vide infra*).

2.2.3. Thioamidine Cyclization. While the formation of thioamidine **22** was straightforward, subsequent ring closure under acid catalysis (Ghosez's reagent, methanesulfonic and trifluoroacetic acids) was complicated by the formation of up to 20% of oxamidine **25** (Scheme 3). In light of the competing cyclization driven by the hydroxyl group as a nucleophile, we envisioned that this pathway could be blocked by forming bis-benzoyl isothiocyanate adduct **23** via the addition of two equivalents of BzNCS such that the sulfur-mediated nucleophilic displacement of the BzNHC(S)O group becomes the predominant pathway for cyclization. During the reaction, **22** was observed to form initially as an intermediate and then slowly (6 h at RT) converted to **23**. Upon heating the reaction mixture, **2a** was generated as a major product. Using this method, the oxamidine byproduct **25** was reduced to less than 3% and was fully rejected during crystallization of the product. This protocol worked sufficiently well for delivery of the first two campaigns (4.4 and 25 kg, respectively). In the third campaign, however, we employed an improved process developed by DeBaillie and co-workers[14] for an analogous transformation, in which 1 equiv of CDI was used to convert **22** to **24**, and subsequent heating gave **2a** with a cleaner reaction profile. The use of CDI helped reduce stoichiometry of odorous BzNCS to 1.0 equiv, although oxamidine **25** was still present at similar levels in the reaction mixture. While **2a** is a crystalline solid, the product isolation by crystallization incurred substantial loss in all solvent systems examined. The crude product was therefore telescoped directly into the next step.

2.2.4. Deprotection of the Boc Group to Form 2. When crude **2a** was subjected to the Boc deprotection reaction by treatment with conc. HCl, the HCl salt of **2a** unexpectedly crystallized from ethyl acetate with the Boc group intact. This offered a great opportunity for impurity purge and allowed isolation of **2a·HCl** in high purity and yield. Robustness of the HCl salt formation was ensured as up to 2 equiv of concn HCl (aq) solution at RT could be tolerated and resulted in no sign of Boc removal. Deprotection of the Boc group from **2a·HCl** was readily effected with methanolic HCl solution (6 equiv). Surprisingly, the isolation of **2** as a free base or HCl salt turned out to be a challenge. Direct quench of the Boc deprotection reaction by adding a base led to product decomposition that was not fully understood. Nevertheless, inverse quench by adding the reaction mixture to an agitated mixture of aqueous

https://doi.org/10.1021/acs.oprd.1c00126
Org. Process Res. Dev. 2021, 25, 1440−1453

Scheme 4. Endgame Synthesis of 1[a]

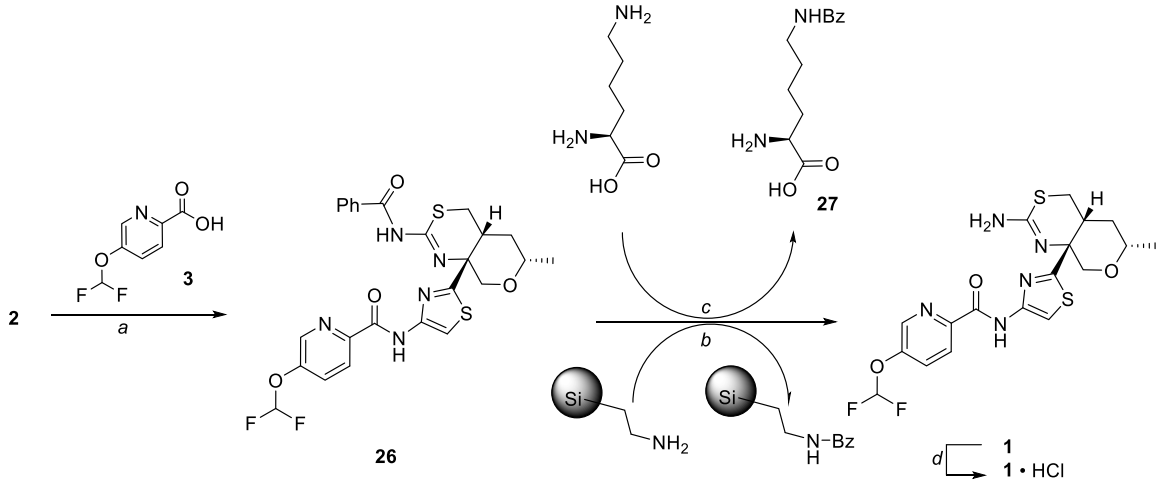

[a]Reagents and conditions: (a) T_3P, EtOAc, RT; iPrOH, aq HCl, 93%; (b) Silicycle-diamine, DCM/THF, 93%; (c) L-lysine, 1-PrOH, water, 90 °C; aq NaOH; 86%. (d) aq HCl, MEK, 87%.

base (Na_2HPO_4 or TEA) and organic solvent (EtOAc) addressed the problem.

2.3. Endgame Development. *2.3.1. Amidation Reaction.* The coupling of hydropyranothiazine **2** with 5-(difluoromethoxy)picolinic acid (**3**) was straightforward (Scheme 4) with the use of propane phosphonic acid anhydride (T_3P solution in ethyl acetate) as the coupling reagent. The product isolation was streamlined with the addition of aqueous HCl and isopropanol, which resulted in direct product crystallization. Upon removal of ethyl acetate by concentration, the product (**26**) was isolated in 95% yield. The process was robust as it offered great opportunities to purge most incoming impurities from **2a**, notably a carried forward impurity from des-bromo compound (**15**) that might be present in the starting material.[15] The reaction was found readily adaptable to a continuous flow process, which was demonstrated in the laboratory using either T_3P or EDC/HOPO as coupling reagents to give comparable yields and quality,[16] although a batch approach was implemented for initial manufacturing.

2.3.2. Benzamide Deprotection. Deprotection of the benzamide group from **26** required differentiation (Scheme 4) between the benzamide and picolinamide. Methoxyamine was identified initially, and it offered high selectivity, but the byproduct *N*-methoxybenzamide could not be easily rejected as it cocrystallized with the desired product. To circumvent this issue, the use of SiliaMet Diamine (Si-DIA) was explored; it was found to be highly chemoselective and gave an extremely clean reaction profile. The workup was straightforward by simply removing the silica gel by filtration as the benzoyl group coming off **26** was solid-phase bound. This protocol was employed in the first and second campaigns to give 86−88% yield of **1**. With the increased clinical demand, we recognized that the use of Si-DIA was not a long-term option due to its relatively high cost. Thus, alternative methods were investigated. Nucleophilic amines (*n*-butylamine, pyrrolidine, and piperidine) were found to offer reasonable chemoselectivity. However, the corresponding amide byproducts were difficult to remove in the product isolation. With this in mind, we envisioned that a water-soluble amine could be the answer. Thus, L-lysine, an inexpensive commodity chemical, fit the requirements perfectly; the Bz-Lysine byproduct **27** is water-soluble so it could be expediently rejected in the aqueous workup under appropriate pH. The reaction was carried out in *n*PrOH/water at reflux. Upon reaction completion, water was added, followed by a heat/cool cycle to help particle size growth of the crystalline product (**1**) to facilitate the filtration. The pH was then adjusted by the addition of aqueous NaOH to allow for the removal of **27**, its residual level was found to be critical on the overall filtration time of the reaction mixture. The basic aqueous isopropanol mixture was noted to be quite viscous at cool temperature (0 to 20 °C), which dramatically slowed down the filtration. By increasing the temperature of prefiltered slurry to 40 °C, the filtration proceeded much speedily. With those improvements, the filtrate rate was increased by nearly 50-fold; in a 67 kg batch, the filtration was completed in 2 h, and the product was isolated in 86% yield with 99.6% purity.

2.3.3. Final HCl Salt Formation. As the mono-hydrochloride salt was selected for clinical development, the final processing involved an HCl salt formation. HCl (aq) was used in combination with methyl ethyl ketone; the protocol offered good recovery of **1**·HCl as a crystalline product in excellent purity.

3. SUMMARY

The development of an efficient synthetic process for manufacture of thiazolyl hydropyranoisoxazole (**4**) has been successfully achieved. The CSTR process established a robust and reliable platform for scalable synthesis featuring a continuous Li−Br exchange reaction, followed by the addition of the lithiothiazole to the isoxazolene (**5**). By taking advantage of significant modifications of the first-generation process to avoid issues with gelling, in conjunction with developing a methanesulfonic acid salt formation for product isolation, the overall efficiency of the synthesis and the product quality was dramatically improved, resulting in 78−80% isolated yield with 99% purity at up to the 70 kg scale. The CSTR continuous flow process exhibited significant advantages over the batch process in terms of yield, product quality, and risk management. A gravity overflow design obviated the need for multiple pumping mechanisms for transfer of the heterogeneous

https://doi.org/10.1021/acs.oprd.1c00126
Org. Process Res. Dev. 2021, 25, 1440−1453

reaction mixture. It is noteworthy that the cooling capacity of the jacketed CSTRs was a key factor impacting process efficiency for these highly exothermic lithiation and anion addition reactions to prepare the isoxazolene. The subsequent sequence of the synthesis was successfully developed, most notably with the novel use of SiliaMet Diamine and L-lysine for the deprotection of the benzamide group, which allowed convenient isolation of the product.

4. EXPERIMENTAL SECTION

4.1. General. NMR chemical shifts are reported in parts per million (ppm) with TMS as an internal standard. Reagents and solvents were obtained from commercial sources and used without further purifications. The reactions were monitored offline by UPLC or HPLC during the laboratory development and continuous flow production. UPLC method: Agilent SB-CN column (2.1 × 50 mm) with mobile phases A (0.05% TFA in water) and B (acetonitrile). Detection wavelength 210 nm; flow rate 0.65 mL/min, 0−2.9 min, ramp from 5% B to 100% B; 2.9−3.4 min, stay at 100% B; 3.4−3.5 min, ramp to 5% B; 3.5−4.0 min, 5% B. HPLC method: Zorbax Eclipse Plus C18 column; (4.6 × 100 mm; 3.5 μm, P/N: 959961-902) at 40 °C with mobile phases A (0.1% H_3PO_4 in water) and B (acetonitrile). Detection wavelength 210 nm; flow rate 1.5 mL/min, 0−8 min, ramp from 10% B to 60% B; 8−11 min, ramp to 95% B; 11−13 min, stay at 95% B; 13−16 min, ramp to 10% B. Chiral HPLC method: Chiralpak AD-H, 250 × 4.6 mm, 5 μm, column temperature 30 °C. Flow rate 1.0 mL/min; mobile phase isocratic 60% *n*-hexane/40% EtOH with 0.05% diethylamine, run time 19 min. GC method: column RTX1701, 30 m × 0.32 mm ID × 1.0 μm film, Inlet temperature is 250 °C; 160.0 kPa pressure; helium gas flow rate 6.5 mL/min; detector temperature 270 °C; nitrogen as make up gas H_2/air/N_2 = 40:450:30 (mL/min); equilibration time 0.5 min; injection volume 1 mL; run time 17 min. Temperature gradient: rate 25 °C/min, final temperature 250 °C, final time 4 min.

*4.1.1. tert-Butyl (2-((3aR,5S,7aR)-5-Methyltetrahydro-1H-pyrano[3,4-c]isoxazol-7a(7H)-yl)thiazol-4-yl)carbamate (**4**).* *4.1.1.1. Batch Mode.* A clean and dry 1500 L titanium reactor was evacuated to −0.05 to −0.08 MPa and then filled with nitrogen to normal pressure. This was repeated three times. Toluene (210 kg) was charged into the reactor and a sample was pulled to confirm KF ≤0.03%. The mixture was cooled to −85 to −75 °C. 2.5 M *n*-BuLi solution in *n*-hexane solution (63.0 kg, 227 mol, 90.9 L) was added at −85 to −75 °C. To this reactor was added slowly a solution of 2,4-dibromothiazole (54.0 kg, 222 mol) in a solvent mixture of toluene (210 kg) and THF (210 kg) that was prepared in a separate reactor and held at 0−10 °C. During the transfer, the 1500 L titanium reactor was maintained at −79 to −70 °C, and the addition time was 7 h 57 min. After the addition was complete, the reaction mixture was sampled by quenching a sample aliquot into an ammonium chloride solution and checked by HPLC to confirm that the Li−Br exchange was complete. To this reaction mixture was then slowly added a solution mixture of isoxazolene **5** (24.5 kg, 173 mol) and boron trifluoride etherate (32.3 kg, 286 mol) in THF (210 kg) that was previously prepared. During the transfer, the 1500 L titanium reactor was maintained at −85 to −70 °C. The transfer time was 3 h 23 min. 1 h after the transfer was complete, the reaction was confirmed to be complete, and the reaction mixture was warmed to −10 °C and quenched with 20% ammonium chloride solution (175 kg). The mixture was warmed to 15−25 °C and filtered through a celite pad to remove insoluble materials. The filter cake was rinsed with toluene (78 kg). The organic phase of the filtrate was separated and washed with aq 12% sodium carbonate solution (50 kg), followed by 10% aq sodium chloride (132 kg). The organic phase was concentrated at ≤45 °C under reduced pressure ≤−0.08 MPa until 50−75 L of the mixture remained. Then, acetonitrile (120 kg) was added into the mixture. Then, it was sampled for toluene residual by GC analysis until toluene residual ≤20%. The mixture was cooled to 0−10 °C; then, methanesulfonic acid (16.9 kg, 176 mol) was added into the mixture. The mixture was stirred at 5−10 °C to induce crystallization and held for 2−4 h. The mixture was filtered, and the filter cake was rinsed with acetonitrile (47.0 kg). The wet filter cake (**4**-MSA) was combined with methanol (198 kg) in a reactor and stirred until the solid dissolved. It was then cooled to 15 °C. 2.3% sodium hydroxide solution (300 kg) was added, and the pH analysis was confirmed at >9. The mixture was concentrated at ≤45 °C under reduced pressure ≤−0.08 MPa until ∼400 L remained. The mixture was sampled for methanol residual at ≤15%. The mixture was cooled to 10 °C and stirred for 3 h. The mixture was filtered and the filter cake was rinsed with purified water (60.0 kg × 2). The filter cake was vacuum oven-dried at 25−35 °C until KF reached ≤1.0% and methanol residual reached ≤0.5%. 34.0 kg gross weight (33.5 kg corrected for potency, 63.2% yield) product **4** was isolated as a light-yellow solid (achiral purity 98.4%; chiral purity 99.0%). The spectroscopic data were identical to those reported in the literature.[3b]

4.1.1.2. CSTR Continuous Flow Mode. Pump A. Directly feeding from anhydrous toluene as a solvent line.

Pump B. Directly feeding from 23 wt % *n*-BuLi solution in hexane.

Pump C feed preparation. A dry and clean 500 L glass-lined reactor was nitrogen purged. Toluene (204 kg) was added to the reactor and the mixture was sampled for KF analysis until KF ≤0.03%. At 15−30 °C, 2,4-dibromothiazole (79.0 kg, 325 mol) was added into the mixture and stirred until the solid dissolves completely by visual check (this feed solution was made up twice to support one continuous run).

Pump D feed preparation. Anhydrous THF (70.2 kg) was added into the 3000 L glass-lined reactor and the mixture was sampled to confirm KF ≤0.05%. Additional THF (615 kg) was added, and the internal temperature was maintained at 15−30 °C. Isoxazolene **5** (70.0 kg, 496 mol) was added and stirred until a solution was obtained. Borontrifluoride etherate (94.6 kg, 838 mol) was added into the abovementioned mixture at 15−30 °C. After addition, the mixture was stirred for 0.5−1 h and held for use.

4.1.1.3. Cooling of the CSTR Prior to Start. The first- and second-stage CSTR jacket temperature were cooled to −70 to −90 °C and the third-, fourth-, and fifth-stage CSTR jacket temperatures were cooled to −60 to −75 °C and then maintained for at least 0.5−1 h.

4.1.1.4. Setup of Pump Flow Rates. The flow rate of feed pump A was set at 141.0 g/min, pumps B at 45.0 g/min, pump C at 181.5 g/min, and pump D at 199.5 g/min. The adjusting solvent was toluene (59.5 kg). When toluene was pumped into the fifth-stage CSTR, the mixture was sampled from the lower port of the fifth-stage CSTR for KF analysis until KF ≤0.03%.

4.1.1.5. Receiving Tank. 0−10 °C ammonium chloride (70.0 kg) solution in water (2309 kg).

https://doi.org/10.1021/acs.oprd.1c00126
Org. Process Res. Dev. 2021, 25, 1440−1453

4.1.1.6. System Startup and Shutdown. The jacket temperatures of the CSTRs were achieved to the specified ranges *vide supra*. Both pumps A and B were started simultaneously. Feed pump C was timed to be switched on when CSTR-1 was about to overflow to CSTR-2, which was ∼60 min after the start of pumps A and B. Approximately 20 min after the start of pump C, feed pump D was switched on. The reaction was monitored by HPLC analysis at CSTR-2 for the conversion of **6** and at CSTR-5 for both the conversion of **5** and the formation of **4**. Upon completion of solution D feeding, all pumps were stopped, and the CSTRs were stirred for 0.5−1 h at −55 to −65 °C. The contents of the last three CSTRs were transferred to the receiving tank, and the first two CSTRs were diverted to a separate quench container for disposal. The combined quenched reaction mixture was filtered through a celite pad (20 kg), and the resulting mixture was phase-separated. The organic phase was washed with sodium carbonate (18.0 kg) solution in water (341 kg), followed by saturated brine solution (385 kg). The resulting organic phase was fully concentrated under partial vacuum. Acetonitrile (343 kg) was added, and the resulting solution was cooled to 0−10 °C. Methanesulfonic acid (47.7 kg, 496 mol) was added slowly, and the resulting mixture was stirred for 1−3 h at 5−10 °C to induce crystallization. Upon further stirring for 1−2 h at the same temperature, the slurry was filtered, and the filter cake was rinsed with acetonitrile (4 × 34 kg). The resulting wet filter cake as a crude **4-MSA** salt was combined with methanol (560 kg) at 5−15 °C. Aqueous sodium chloride (20 kg) in water (848 kg) was added. The resulting mixture was concentrated under vacuum until the total volume reached ∼1000 L and then stirred at 0−10 °C for ∼2 h. The resulting slurry was filtered and rinsed with water (5 × 58 kg). The filter cake was dried under vacuum at 25−35° for 12 h to give **4** as a light-brown solid (67.4 kg 78.1%) in HPLC purity 99.4% (KF 0.4%. qNMR potency 97.4%). The spectroscopic data were identical to those reported in the literature.[3b]

*4.1.2. tert-Butyl (2-((3aR,5S,7aR)-5-Methyltetrahydro-1H-pyrano[3,4-c]isoxazol-7a(7H)-yl)thiazol-4-yl)carbamate (**4a**).* A dry and nitrogen-purged 2000 L glass-lined reactor was charged with toluene (984 kg), and the reactor was evacuated three times and refilled with nitrogen, followed by cooling to 15−30 °C. **4** (112.5 kg, 368.6 mol), *tert*-butyl carbamate (106.1 kg, 905.6 mol), and potassium carbonate (151.3 kg, 1095 mol) were added to the mixture. The mixture was evacuated to ∼−0.08 MPa and filled with nitrogen. This was repeated five times. The reactor was sampled for oxygen content to ensure it was ≤400 ppm. A mixture of tris(dibenzylideneacetone)dipalladium (29.9 kg, 3.26 mol) and 2-di-*t*-butylphosphino-2′,4′,6′-tri-*i*-propyl-1,1′-biphenyl (7.80 kg, 18.4 mol) was added to the reaction mixture under protection of nitrogen. The resulting reaction mixture was heated at reflux for 5 h upon reaction completion confirmed by HPLC sampling. The mixture was cooled to 20 °C, and THF (399 kg) was added. The resulting mixture was filtered and the filter cake washed with THF (380 kg). The combined filtrate was concentrated at ≤55 °C under reduced pressure (−0.08 MPa) until ∼250 L of the mixture remained. The mixture was cooled to 25−35 °C, and THF (191 kg) was added. The total weight of the final solution was 446 kg (100% yield assumed), and it was carried over to the next step. This step was repeated three times on similar scales.

*4.1.3. tert-Butyl (2-((3R,4R,6S)-3-Amino-4-(hydroxymethyl)-6-methyltetrahydro-2H-pyran-3-yl)thiazol-4-yl)-carbamate (**21**).* A dry and nitrogen-purged 3000 L autoclave reactor was charged with Raney-nickel (64.6 kg) under nitrogen. The reactor was again evacuated and purged with nitrogen five times. At 15−25 °C, isopropanol (814 kg) and the abovementioned crude **4a** solution (514 kg of THF solution 129 kg by potency, 378 mol) were charged to the reactor with the agitation off. The agitation was then started and argon was bubbled from the bottom of the reactor for 20 min. While maintaining at 15−35 °C, the reaction mixture was purged with argon to 0.15−0.2 MPa and then vented to 0.05 MPa; the purge and vent operation was repeated five times. The reactor was sampled for oxygen content to ensure it was ≤0.1%. At 15−25 °C, the resulting mixture was purged with hydrogen to 0.3−0.5 MPa and then vented to 0.05 MPa; the purge and vent operation was repeated five times. The pressure was then increased to 0.35−0.5 MPa with hydrogen. The mixture was maintained at 25−35 °C under 0.35−0.5 MPa for 8 h, and HPLC analysis showed reaction completion. The mixture was purged with argon to 0.15−0.2 MPa and vented to 0.05 MPa. This was repeated five times. The mixture was filtered over celite (14.6 kg), and the reactor wall and filter cake were rinsed with isopropanol (410 kg). The combined filtrate was concentrated at ≤45 °C under reduced pressure until ∼270 L remained. The mixture was cooled to 20−30 °C, and dichloromethane (969 kg) was added. At 20−30 °C, the pH of the mixture was adjusted to 2.5−3.0 with aqueous citric acid (prepared by mixing 411 kg of citric acid in 2067 kg of water). The organic phase was extracted with the above-mentioned pre-prepared citric acid solution (895 kg). The product-rich, combined aqueous phase was mixed with ethyl acetate (1154 kg), and the pH of the aqueous phase was adjusted to ∼8 with a solution of potassium carbonate (527 kg) in purified water (649 kg) at a rate of 10−30 kg/h. The biphasic mixture was filtered through celite (12.6 kg), and the filter cake was rinsed with ethyl acetate (465 kg). The phases were separated, and the organic phase was concentrated at ≤45 °C under reduced pressure until 220−260 L remained. The resulting solution was solvent-exchanged with THF (3 × 450 kg) at ≤45 °C under reduced pressure until 220−260 L of the mixture remained. The mixture was sampled for until KF ≤0.1%. The mixture was cooled to 15−25 °C. THF (220 kg) was added to give a solution of **21** in gross weight 564 kg (89.3 kg product corrected for potency, 260 mol, 68.8%). The resulting solution was directly carried forward to the next step. This step was repeated three times on similar scales. The spectroscopic data were identical to those reported in the literature.[3c]

*4.1.4. tert-Butyl (2-((4aR,6S,8aR)-2-Benzamido-6-methyl-4,4a,5,6-tetrahydropyrano[3,4-d][1,3]thiazin-8a(8H)-yl)-thiazol-4-yl)carbamate Hydrochloride (**2a·HCl**).* A dry and nitrogen-purged 3000 L glass-lined reactor was charged with THF (306 kg) and 562 kg of crude **21** solution (84.5 kg corrected for potency, 246 mol). The mixture was sampled for KF at ≤0.1%. The mixture was heated to 48−60 °C, benzoyl isothiocyanate solution which was prepared with benzoyl isothiocyanate (40.9 kg, 250 mol) and THF (158.0 kg) was added into the mixture with a peristaltic pump in 3 h. The mixture was reacted at 48−60 °C for 3 h and then sampled by HPLC analysis to confirm that the formation of intermediate **22** was complete. While maintaining the temperature at 48 to 60 °C, 1,1′-carbonyldiimidazole (43.4 kg, 268 mol) was added. The mixture was heated at 48 to 60 °C for 24 h, and the reaction was deemed complete by HPLC analysis. The mixture

https://doi.org/10.1021/acs.oprd.1c00126
Org. Process Res. Dev. 2021, 25, 1440−1453

was cooled to 20 to 35 °C and concentrated at ≤45 °C under reduced pressure ($P \leq -0.08$ MPa) until ∼160 L remained. The resulting mixture was solvent-exchanged with ethyl acetate (378 kg) until THF residual reached ≤5%. Ethyl acetate (899 kg) was added. While maintaining at 15−30 °C, citric acid solution which was prepared with citric acid (89.5 kg) and purified water (803 kg) was added into the mixture, and the resulting phases were separated. The organic phase was washed with 15% sodium chloride solution (480 kg) and then concentrated at ≤45 °C under reduced pressure ($P \leq -0.08$ MPa) until ∼450 L remained. The resulting mixture was cooled to −10 to 0 °C. While maintaining at this temperature, aq HCl solution which was prepared with conc. HCl (38.0 kg) and water (74 kg) was added into the mixture. The resulting mixture was stirred at −10 to 0 °C for 6 h, and the resulting slurry was filtered with a centrifuge and the filter cake was washed with ethyl acetate (3 × 51 kg) and then with water (5 × 85 kg). The filter cake was dried in a rotary conical dryer at 30−60 °C under reduced pressure ($P \leq -0.08$ MPa) until KF was ≤0.5% and ethyl acetate ≤2.0%, respectively. Product **2a·HCl** was isolated as a yellow solid (112.7, 106.6 kg corrected for potency, 82.2%). This step was repeated two times on similar scales. LCMS m/z (M + 1): 489.2, 354.3, 175.1, 103.1 ^{1}H NMR (DMSO-d_6, 400 MHz): δ 10.27 (br 1s),8.15 (d, J = 8.0 Hz, 2H), 7.68−7.62 (m, 1H), 7.58−7.51 (m, 2H), 7.25 (s, 1H), 4.09−3.98 (m, 1H), 3.84−3.60 (m, 2H), 3.12−2.82 (m, 3H), 1.78−1.72 (m, 1H), 1.65−1.36 (m, 10H), 1.26−1.15 (m, 3H).

*4.1.5. N-((4aR,6S,8aR)-8a-(4-Aminothiazol-2-yl)-6-methyl-4,4a,5,6,8,8a-hexahydropyrano[3,4-d][1,3]thiazin-2-yl)-benzamide (**2**).* A dry and nitrogen-purged 1000 L glass-lined reactor was charged with methanol (316 kg). The reactor was cooled to 0−10 °C. While maintaining at this temperature, acetyl chloride (121.5 kg, 1548 mol) was added slowly. After addition, the resulting mixture was stirred for 2 h and then warmed to 25−30 °C. **2a·HCl** (136.6, 130.1 kg corrected for potency, 247.7 mol) was added into the mixture in portions. The solid addition funnel and reactor wall were rinsed with methanol (14 kg). The resulting reaction mixture was stirred at 20−30 °C for 4 h, and at this point, the reaction was confirmed to be complete by HPLC analysis. While maintaining the temperature at 0−30 °C, the mixture was inversely quenched into a mixture of ethyl acetate (1794 kg), purified water (2027 kg), and triethylamine (272.2 kg) that was precooled to 0−10 °C. The mixture was warmed to 20−30 °C, and the phases were separated. The aqueous phase was backextracted with ethyl acetate (2 × 480 kg) once. The combined organic phase was washed with water (4 × 1350 kg) and then concentrated at ≤45 °C under reduced pressure ≤−0.08 MPa until ∼220 L remained. At 30−40 °C, methanol (33.0 kg) and MTBE (1003 kg) were added, and the resulting slurry was stirred at 20−30 °C for 2 h and then cooled to 0−10 °C. The mixture was filtered with a stainless-steel nutsche filter; the filter cake was rinsed with MTBE (100 kg). The filter cake was dried in a rotary conical dryer at 35 to 45 °C under reduced pressure ($P \leq -0.08$ MPa) until both ethyl acetate residue and MTBE residue reached ≤0.5%. Product **2** was isolated as a light-brown solid (69.0, 67.6 kg corrected, 70.2%) in 100% HPLC purity (98% potency). This step was repeated two times on similar scales. The spectroscopic data were identical to those reported in the literature.[3b]

*4.1.6. N-(2-((4aR,6S,8aR)-2-Benzamido-6-methyl-4,4a,5,6-tetrahydropyrano[3,4-d][1,3]thiazin-8a(8H)-yl)thiazol-4-yl)-5-(difluoromethoxy)picolinamide (**26**).* A dry and nitrogen-purged reactor with jacket temperature at 15−25 °C was charged with ethyl acetate (124 kg), followed by **3** (13.0 kg, 67.2 mol). The resulting mixture was stirred for 30 min and then cooled to 10 °C. Triethylamine (27.5 kg, 272 mol) was added, followed by the addition of **2** (24.8 kg, 63.6 mol). The reaction was cooled to 0 °C. 50% T_3P solution in ethyl acetate (102 kg, 160 mol) was slowly added to the reaction while maintaining the reaction temperature below 5 °C. After the addition, the reaction was warmed to 25 °C and held for 12 h. The reaction was then cooled to 10 to 15 °C, and isopropanol (115 kg) was added, followed by the addition of 0.5 N aq HCl (99 kg). The resulting mixture was concentrated to ∼350 L under atmospheric pressure, then cooled to 0 to 10 °C over 3 h, and held at this temperature for 6 h. The resulting slurry was filtered, and the filter cake was rinsed with a 1:1 volumetric mixture of isopropanol (39.3 kg)/water (50 kg). The filter cake was dried at 50 °C under vacuum ($P \leq -0.08$ MPa) to give the desired product as an off-white solid (34.0, 33.2 kg for potency, 59.3 mol, 93.2%) in 99% UPLC purity. The spectroscopic data were identical to those reported in the literature.[3b]

*4.1.7. N-(2-((4aR,6S,8aR)-2-Amino-6-methyl-4,4a,5,6-tetrahydropyrano[3,4-d][1,3]thiazin-8a(8H)-yl)thiazol-4-yl)-5-(difluoromethoxy)picolinamide (**1**).* A nitrogen-purged reactor with jacket temperature at 25 °C was charged with **30** (32.5 kg, 58.1 mol), 1-propanol (154 kg), and water (65 kg). L-lysine (46.7 kg, 319 mol, 5.5 equiv) was then added. The resulting mixture was heated at 90 °C for 24 h. When the reaction was confirmed complete, it was cooled to 55 °C over 30 min, and 3.2 N aq NaOH solution (100 kg) was added slowly. After the addition was complete, the reaction mixture was cooled to 25 °C in 2 h. The resulting slurry was heated to 55 °C, then cooled to 20 °C in a 2 h cycle to increase the particle size, and then concentrated at ∼40 °C under vacuum (110 mbar) to ∼230 L. Water (130 kg) was added slowly over 1 h at the same temperature, and the agitation was continued at 40 °C for 1 h and then cooled to 20 °C. The resulting slurry was filtered, and the filter cake was rinsed with a 7:1 volumetric ratio of water/1-propanol (2 × 63 kg). The filter cake was dried at 50 °C under vacuum ($P \leq -0.08$ MPa) to give the desired product which was a white solid (22.9 kg, 50.3 mol, 86.4%) in 99.6% UPLC purity. The spectroscopic data were identical to those reported in the literature.[3b]

*4.1.8. N-(2-((4aR,6S,8aR)-2-Amino-6-methyl-4,4a,5,6-tetrahydropyrano[3,4-d][1,3]thiazin-8a(8H)-yl)thiazol-4-yl)-5-(difluoromethoxy)picolinamide (**1·HCl**).* A nitrogen-purged reactor with jacket temperature at 25 °C was charged with 2 (22.8 kg, 500 mol) and MEK (238 kg). The resulting mixture was heated to 45 to 55 °C for ∼1 h, and a complete solution was obtained. The resulting solution was held at 45 to 55 °C, filtered through a 0.5 μm in-line cartridge filter, and rinsed with MEK (18 kg). To the filtrate that was cooled to 30 to 40 °C was added a solution of aq HCl solution in MEK prepared by combining 120 kg of 5 N aq HCl (600 mol, 1.2 equiv) and 110 kg of MEK, while maintaining at 30 to 40 °C. After the addition was complete, the reaction mixture was stirred at 30 to 40 °C for >2 h and then cooled to 0 to 10 °C over 3 h. The resulting slurry was filtered and rinsed with MEK (55 kg). The filter cake was dried at 50 °C under vacuum ($P \leq -0.08$ MPa) to give the desired product as a white solid (21.5 kg, 87.2%) in 99.8% UPLC purity. The spectroscopic data were identical to those reported in the literature.[3b]

https://doi.org/10.1021/acs.oprd.1c00126
Org. Process Res. Dev. 2021, 25, 1440−1453

AUTHOR INFORMATION

Corresponding Author

Bryan Li − *Chemical Research & Development, Worldwide Research Development & Medical, Pfizer Inc., Groton, Connecticut 06340, United States; Chemical Research & Development La Jolla Laboratory, Worldwide Research Development & Medical, Pfizer Inc., San Diego, California 92121, United States;* orcid.org/0000-0002-7972-9966; Email: bryan.li@pfizer.com

Authors

Richard W. Barnhart − *Chemical Research & Development, Worldwide Research Development & Medical, Pfizer Inc., Groton, Connecticut 06340, United States;* orcid.org/0000-0002-7666-8942

Amelie Dion − *Chemical Research & Development, Worldwide Research Development & Medical, Pfizer Inc., Groton, Connecticut 06340, United States;* Present Address: Merck and Co. Rahway, New Jersey, United States.

Steven Guinness − *Chemical Research & Development, Worldwide Research Development & Medical, Pfizer Inc., Groton, Connecticut 06340, United States*

Alan Happe − *Chemical Research & Development Worldwide Research Development & Medical, Pfizer Inc., Sandwich CT13 9ND, U.K.*

Cheryl M. Hayward − *Chemical Research & Development, Worldwide Research Development & Medical, Pfizer Inc., Groton, Connecticut 06340, United States*

Jeffrey Kohrt − *Chemical Research & Development, Worldwide Research Development & Medical, Pfizer Inc., Groton, Connecticut 06340, United States*

Teresa Makowski − *Chemical Research & Development, Worldwide Research Development & Medical, Pfizer Inc., Groton, Connecticut 06340, United States*

Mark Maloney − *Chemical Research & Development, Worldwide Research Development & Medical, Pfizer Inc., Groton, Connecticut 06340, United States*

Jade D. Nelson − *Chemical Research & Development, Worldwide Research Development & Medical, Pfizer Inc., Groton, Connecticut 06340, United States*

Asaad Nematalla − *Chemical Research & Development, Worldwide Research Development & Medical, Pfizer Inc., Groton, Connecticut 06340, United States*

J. Christopher McWilliams − *Chemical Research & Development, Worldwide Research Development & Medical, Pfizer Inc., Groton, Connecticut 06340, United States;* orcid.org/0000-0002-4764-735X

Zhihui Peng − *Chemical Research & Development, Worldwide Research Development & Medical, Pfizer Inc., Groton, Connecticut 06340, United States*

Jeffrey Raggon − *Chemical Research & Development, Worldwide Research Development & Medical, Pfizer Inc., Groton, Connecticut 06340, United States*

John Sagal − *Chemical Research & Development, Worldwide Research Development & Medical, Pfizer Inc., Groton, Connecticut 06340, United States*

Gerald A. Weisenburger − *Chemical Research & Development, Worldwide Research Development & Medical, Pfizer Inc., Groton, Connecticut 06340, United States*

Denghui Bao − *Asymchem Life Science Co. Limited, Tianjin 300457, China*

Miguel Gonzalez − *Asymchem Life Science Co. Limited, Tianjin 300457, China;* Present Address: Alcon, Fort Worth, Texas, United States.

Jiangping Lu − *Asymchem Life Science Co. Limited, Tianjin 300457, China*

Mark D. McLaws − *Asymchem Life Science Co. Limited, Tianjin 300457, China*

Jian Tao − *Asymchem Life Science Co. Limited, Tianjin 300457, China*

Baolin Wu − *Asymchem Life Science Co. Limited, Tianjin 300457, China*

Complete contact information is available at: https://pubs.acs.org/10.1021/acs.oprd.1c00126

Notes

The authors declare no competing financial interest.

[¶]Retired from Pfizer.

ACKNOWLEDGMENTS

We thank Mark Barilla and the staff of Groton Kilo Lab, Sandwich Product Development Facility, and Asymchem Production Plant for their support.

DEDICATION

[⊥]Dedicating this paper to Professor Elie Abushanab on the occasion of his 85th birthday.

REFERENCES

(1) (a) Rauk, A. Why is the amyloid beta peptide of Alzheimer's disease neurotoxic? *Dalton Trans.* **2008**, *10*, 1273−1282. (b) Murphy, M. P.; LeVine, H., 3rd Alzheimer's disease and the amyloid-beta peptide. *J. Alzheimer's Dis.* **2010**, *19*, 311−323. (c) Brothers, H. M.; Gosztyla, M. L.; Robinson, S. R. The Physiological Roles of Amyloid-β Peptide Hint at New Ways to Treat Alzheimer's Disease. *Front. Aging Neurosci.* **2018**, *10*, 118.

(2) (a) Prati, F.; Bottegoni, G.; Bolognesi, M. L.; Cavalli, A. BACE-1 Inhibitors: From Recent Single-Target Molecules to Multitarget Compounds for Alzheimer's Disease. *J. Med. Chem.* **2018**, *61*, 619−637. (b) Vassar, R. β-Secretase (BACE) as a drug target for alzheimer's disease. *Adv. Drug Delivery Rev.* **2002**, *54*, 1589−1602. (c) Vassar, R.; Kandalepas, P. C. The β-secretase enzyme BACE1 as a therapeutic target for Alzheimer's disease. *Alzheimer's Res. Ther.* **2011**, *3*, 20. (d) John, V.; Beck, J. P.; Bienkowski, M. J.; Sinha, S.; Heinrikson, R. L. Human β-Secretase (BACE) and BACE Inhibitors. *J. Med. Chem.* **2003**, *46*, 4625−4630. (e) Oehlrich, D.; Berthelot, D. J.-C.; Gijsen, H. J. M. γ-Secretase Modulators as Potential Disease Modifying Anti-Alzheimer's Drugs. *J. Med. Chem.* **2011**, *54*, 669−698. (f) Bursavich, M. G.; Harrison, B. A.; Blain, J.-F. Gamma Secretase Modulators: New Alzheimer's Drugs on the Horizon? *J. Med. Chem.* **2016**, *59*, 7389−7409. (g) Björklund, C.; Oscarson, S.; Benkestock, K.; Borkakoti, N.; Jansson, K.; Lindberg, J.; Vrang, L.; Hallberg, A.; Rosenquist, A.; Samuelsson, B. Design and Synthesis of Potent and Selective BACE-1 Inhibitors. *J. Med. Chem.* **2010**, *53*, 1458−1464. (h) Ginman, T.; Viklund, J.; Malmström, J.; Blid, J.; Emond, R.; Forsblom, R.; Johansson, A.; Kers, A.; Lake, F.; Sehgelmeble, F.; Sterky, K. J.; Bergh, M.; Lindgren, A.; Johansson, P.; Jeppsson, F.; Fälting, J.; Gravenfors, Y.; Rahm, F. Core Refinement toward Permeable β-Secretase (BACE-1) Inhibitors with Low hERG Activity. *J. Med. Chem.* **2013**, *56*, 4181−4205. (i) Gravenfors, Y.; Viklund, J.; Blid, J.; Ginman, T.; Karlström, S.; Kihlström, J.; Kolmodin, K.; Lindström, J.; von Berg, S.; von Kieseritzky, F.; Slivo, C.; Swahn, B.-M.; Olsson, L.-L.; Johansson, P.; Eketjäll, S.; Fälting, J.; Jeppsson, F.; Strömberg, K.; Janson, J.; Rahm, F. New Aminoimidazoles as β-Secretase (BACE-1) Inhibitors Showing Amyloid-β (Aβ) Lowering in Brain. *J. Med. Chem.* **2012**, *55*, 9297−9311. (j) Mandal, M.; Wu, Y.; Misiaszek, J.; Li, G.; Buevich, A.; Caldwell, J. P.; Liu, X.; Mazzola, R.

D.; Orth, P.; Strickland, C.; Voigt, J.; Wang, H.; Zhu, Z.; Chen, X.; Grzelak, M.; Hyde, L. A.; Kuvelkar, R.; Leach, P. T.; Terracina, G.; Zhang, L.; Zhang, Q.; Michener, M. S.; Smith, B.; Cox, K.; Grotz, D.; Favreau, L.; Mitra, K.; Kazakevich, I.; McKittrick, B. A.; Greenlee, W.; Kennedy, M. E.; Parker, E. M.; Cumming, J. N.; Stamford, A. W. Structure-Based Design of an Iminoheterocyclic β-Site Amyloid Precursor Protein Cleaving Enzyme (BACE) Inhibitor that Lowers Central Aβ in Nonhuman Primates. *J. Med. Chem.* **2016**, *59*, 3231−3248. (k) Huang, H.; La, D. S.; Cheng, A. C.; Whittington, D. A.; Patel, V. F.; Chen, K.; Dineen, T. A.; Epstein, O.; Graceffa, R.; Hickman, D.; Kiang, Y.-H.; Louie, S.; Luo, Y.; Wahl, R. C.; Wen, P. H.; Wood, S.; Fremeau, R. T. Structure- and Property-Based Design of Aminooxazoline Xanthenes as Selective, Orally Efficacious, and CNS Penetrable BACE Inhibitors for the Treatment of Alzheimer's Disease. *J. Med. Chem.* **2012**, *55*, 9156−9169. (l) Gerritz, S. W.; Zhai, W.; Shi, S.; Zhu, S.; Toyn, J. H.; Meredith, J. E.; Iben, L. G.; Burton, C. R.; Albright, C. F.; Good, A. C.; Tebben, A. J.; Muckelbauer, J. K.; Camac, D. M.; Metzler, W.; Cook, L. S.; Padmanabha, R.; Lentz, K. A.; Sofia, M. J.; Poss, M. A.; Macor, J. E.; Thompson, L. A. Acyl Guanidine Inhibitors of β-Secretase (BACE-1): Optimization of a Micromolar Hit to a Nanomolar Lead via Iterative Solid- and Solution-Phase Library Synthesis. *J. Med. Chem.* **2012**, *55*, 9208−9223. (m) Brodney, M. A.; Barreiro, G.; Ogilvie, K.; Hajos-Korcsok, E.; Murray, J.; Vajdos, F.; Ambroise, C.; Christoffersen, C.; Fisher, K.; Lanyon, L.; Liu, J.; Nolan, C. E.; Withka, J. M.; Borzilleri, K. A.; Efremov, I.; Oborski, C. E.; Varghese, A.; O'Neill, B. T. Spirocyclic Sulfamides as β-Secretase 1 (BACE-1) Inhibitors for the Treatment of Alzheimer's Disease: Utilization of Structure Based Drug Design, WaterMap, and CNS Penetration Studies To Identify Centrally Efficacious Inhibitors. *J. Med. Chem.* **2012**, *55*, 9224−9239.

(3) (a) Brodney, M. A.; Beck, E. M.; Butler, C. R.; Barreiro, G.; Johnson, E. F.; Riddell, D.; Parris, K.; Nolan, C. E.; Fan, Y.; Atchison, K.; Gonzales, C.; Robshaw, A. E.; Doran, S. D.; Bundesmann, M. W.; Buzon, L.; Dutra, J.; Henegar, K.; LaChapelle, E.; Hou, X.; Rogers, B. N.; Pandit, J.; Lira, R.; Martinez-Alsina, L.; Mikochik, P.; Murray, J. C.; Ogilvie, K.; Price, L.; Sakya, S. M.; Yu, A.; Zhang, Y.; O'Neill, B. T. Utilizing Structures of CYP2D6 and BACE1 Complexes To Reduce Risk of Drug-Drug Interactions with a Novel Series of Centrally Efficacious BACE1 Inhibitors. *J. Med. Chem.* **2015**, *58*, 3223−3252. (b) O'Neill, B. T.; Beck, E. M.; Butler, C. R.; Nolan, C. E.; Gonzales, C.; Zhang, L.; Doran, S. D.; Lapham, K.; Buzon, L. M.; Dutra, J. K.; Barreiro, G.; Hou, X.; Martinez-Alsina, L. A.; Rogers, B. N.; Villalobos, A.; Murray, J. C.; Ogilvie, K.; LaChapelle, E. A.; Chang, C.; Lanyon, L. F.; Steppan, C. M.; Robshaw, A.; Hales, K.; Boucher, G. G.; Pandher, K.; Houle, C.; Ambroise, C. W.; Karanian, D.; Riddell, D.; Bales, K. R.; Brodney, M. A. Design and Synthesis of Clinical Candidate PF-06751979: A Potent, Brain Penetrant, β-Site Amyloid Precursor Protein Cleaving Enzyme 1 (BACE1) Inhibitor Lacking Hypopigmentation. *J. Med. Chem.* **2018**, *61*, 4476−4504. (c) Brodney, M. A.; Beck, E. M.; Butler, C. R.; Zhang, L.; O'Neill, B. T.; Barreiro, G.; Lachapelle, E. A.; Rogers, B. N. Amides 2-amino-6-méthyl-4,4a,5,6-tétrahydropyrano[3,4-d][1,3]thiazin-8a(8h)-yl-1,3-thiazol-4-yle. WO2015155626 A1, 2015. (d) Garcia-Losada, P.; DeBaillie, A. C.; Eugenio de Diego, J.; Green, S. J.; Hansen, M. M.; Jaramillo, C.; Johnson, M.; Kaoudi, T.; Li, J.; Lindsay-Scott, P. J.; Mateos, C.; Mergott, D. J.; Rincon, J. A.; Rothhaar, R. R.; Seibert, K. D.; Watson, B. M.; Winneroski, L. L.; Gangula, S.; Jing, D.; Sun, H.; Zhang, L.; Frederick, M. O. Synthesis, Optimization, and Large-Scale Preparation of the Low-Dose Central Nervous System-Penetrant BACE1 Inhibitor LY3202626 via a [3 + 2] Nitrone Cycloaddition. *Org. Process Res. Dev.* **2020**, *24*, 306−314. (e) Garcia-Losada, P.; Barberis, M.; Shi, Y.; Hembre, E.; Alhambra Jimenez, C.; Winneroski, L. L.; Watson, B. M.; Jones, C.; DeBaillie, A. C.; Martínez-Olid, F.; Mergott, D. J. Practical Asymmetric Fluorination Approach to the Scalable Synthesis of New Fluoroaminothiazine BACE Inhibitors. *Org. Process Res. Dev.* **2018**, *22*, 650−654. (f) Kolis, S. P.; Hansen, M. M.; Arslantas, E.; Brändli, L.; Buser, J.; DeBaillie, A. C.; Frederick, A. L.; Hoard, D. W.; Hollister, A.; Huber, D.; Kull, T.; Linder, R. J.; Martin, T. J.; Richey, R. N.; Stutz, A.; Waibel, M.; Ward, J. A.; Zamfir, A. Synthesis of BACE Inhibitor LY2886721. Part I. An Asymmetric Nitrone Cycloaddition Strategy. *Org. Process Res. Dev.* **2015**, *19*, 1203−1213. (g) Hansen, M. M.; Jarmer, D. J.; Arslantas, E.; DeBaillie, A. C.; Frederick, A. L.; Harding, M.; Hoard, D. W.; Hollister, A.; Huber, D.; Kolis, S. P.; Kuehne-Willmore, J. E.; Kull, T.; Laurila, M. E.; Linder, R. J.; Martin, T. J.; Martinelli, J. R.; McCulley, M. J.; Richey, R. N.; Starkey, D. R.; Ward, J. A.; Zaborenko, N.; Zweifel, T. Synthesis of BACE Inhibitor LY2886721. Part II. Isoxazolidines as Precursors to Chiral Aminothiazines, Selective Peptide Coupling, and a Controlled Reactive Crystallization. *Org. Process Res. Dev.* **2015**, *19*, 1214−1230. (h) Richardson, J.; Lindsay-Scott, P. J.; Larichev, V.; Pocock, E. Efficient Method for the Synthesis of Amino-1,3-Oxazines from Thioureas. *Org. Process Res. Dev.* **2020**, *24*, 2853−2863. (i) Zaborenko, N.; Linder, R. J.; Braden, T. M.; Campbell, B. M.; Hansen, M. M.; Johnson, M. D. Development of Pilot-Scale Continuous Production of an LY2886721 Starting Material by Packed-Bed Hydrogenolysis. *Org. Process Res. Dev.* **2015**, *19*, 1231−1243. (j) Polster, C. S.; Cole, K. P.; Burcham, C. L.; Campbell, B. M.; Frederick, A. L.; Hansen, M. M.; Harding, M.; Heller, M. R.; Miller, M. T.; Phillips, J. L.; Pollock, P. M.; Zaborenko, N. Pilot-Scale Continuous Production of LY2886721: Amide Formation and Reactive Crystallization. *Org. Process Res. Dev.* **2014**, *18*, 1295−1309.

(4) Qiu, R.; Ahn, J. E.; Alexander, R.; Brodney, M. A.; He, P.; Leurent, C.; Mancuso, J.; Margolin, R. A.; Tankisheva, E.; Chen, D. Safety, Tolerability, Pharmacokinetics, and Pharmacodynamic Effects of PF-06751979, a Potent and Selective Oral BACE1 Inhibitor: Results from Phase I Studies in Healthy Adults and Healthy Older Subjects. *J. Alzheimer's Dis.* **2019**, *71*, 581−595.

(5) We had briefly explored a more convergent approach by lithiating either **6a** or **6b** at the C-2 position as outlined in Scheme 1. While the lithiation proceeded as expected, addition of the resulting anion to isoxazolene **5** was unsuccessful with only trace amount of product detected by UPLC-MS.

(6) We also explored the reversed order of addition, that is, by adding dibromothiazole **6** solution to *n*-BuLi under cryogenic conditions and observed very similar results. Under these conditions, it is believed that dithiothiazole **8** was initially formed as the predominant anion species, which reacted with **6** subsequently to give the mono-lithio anion **7**.

(7) Zeibi Shirejini, S.; Mohammadi, A. Halogen-Lithium Exchange Reaction Using an Integrated Glass Microfluidic Device: An Optimized Synthetic Approach. *Org. Process Res. Dev.* **2017**, *21*, 292−303.

(8) Based on an analogous Li−Br exchange reaction: Zhang, X.; Stefanick, S.; Villani, F. J. Application of Microreactor Technology in Process Development. *Org. Process Res. Dev.* **2004**, *8*, 455−460.

(9) (a) Van Alsten, J. G.; Reeder, L. M.; Stanchina, C. L.; Knoechel, D. J. Continuous Reaction/Crystallization Process for Production of a Hazardous Intermediate. *Org. Process Res. Dev.* **2008**, *12*, 989−994. (b) Kulkarni, A. A.; Kalyani, V. S.; Joshi, R. A.; Joshi, R. R. Continuous Flow Nitration of Benzaldehyde. *Org. Process Res. Dev.* **2009**, *13*, 999−1002. (c) Baumann, M.; Baxendale, I. R.; Martin, L. J.; Ley, S. V. Development of fluorination methods using continuous-flow microreactors. *Tetrahedron* **2009**, *65*, 6611−6625. (d) Baxendale, I. R.; Ley, S. V.; Mansfield, A. C.; Smith, C. D. Multistep Synthesis Using Modular Flow Reactors: Bestmann-Ohira Reagent for the Formation of Alkynes and Triazoles. *Angew. Chem., Int. Ed.* **2009**, *48*, 4017−4021. (e) Li, B.; Widlicka, D.; Boucher, S.; Hayward, C.; Lucas, J.; Murray, J. C.; O'Neil, B. T.; Pfisterer, D.; Samp, L.; VanAlsten, J.; Xiang, Y.; Young, J. Telescoped Flow Process for the Syntheses of N-Aryl Pyrazoles. *Org. Process Res. Dev.* **2012**, *16*, 2031−2035. (f) Li, B.; Bader, S.; Guinness, S. M.; Ruggeri, S. G.; Hayward, C. M.; Hoagland, S.; Lucas, J.; Li, R.; Limburg, D.; McWilliams, J. C.; Raggon, J.; Van Alsten, J. Continuous flow aminolysis under high temperature and pressure. *J. Flow Chem.* **2020**, *10*, 145−156.

(10) For examples of metal-halogen exchange under PFR process, see: (a) von Keutz, T.; Williams, J. D.; Kappe, C. O. Continuous Flow C-Glycosylation via Metal−Halogen Exchange: Process Understanding and Improvements toward Efficient Manufacturing of

https://doi.org/10.1021/acs.oprd.1c00126
Org. Process Res. Dev. 2021, 25, 1440−1453

Remdesivir. *Org. Process Res. Dev.* **2020**, *24*, 2362−2368. (b) Gross, T. D.; Chou, S.; Bonneville, D.; Gross, R. S.; Wang, P.; Campopiano, O.; Ouellette, M. A.; Zook, S. E.; Reddy, J. P.; Moree, W. J.; Jovic, F.; Chopade, S. Chemical Development of NBI-75043. Use of a Flow Reactor to Circumvent a Batch-Limited Metal−Halogen Exchange Reaction. *Org. Process Res. Dev.* **2008**, *12*, 929−939. (c) Kopach, M. E.; Cole, K. P.; Pollock, P. M.; Johnson, M. D.; Braden, T. M.; Webster, L. P.; McClary Groh, J.; McFarland, A. D.; Schafer, J. P.; Adler, J. J.; Rosemeyer, M. Flow Grignard and Lithiation: Screening Tools and Development of Continuous Processes for a Benzyl Alcohol Starting Material. *Org. Process Res. Dev.* **2016**, *20*, 1581−1592. (d) Yu, M.; Strotman, N. A.; Savage, S. A.; Leung, S.; Ramirez, A. A Practical and Robust Multistep Continuous Process for Manufacturing 5-Bromo-N-(tert-butyl)pyridine-3-sulfonamide. *Org. Process Res. Dev.* **2019**, *23*, 2088−2095.

(11) The T-mixer had a narrow channel designed for enhanced mixing, and possibility was the nucleation point when **6** in toluene entered the T-mixer.

(12) The contents did not contain any solid granules, but it appeared to contain small amount of gel material that did not affect the fluidity.

(13) The desired product could be taken to an acidic aqueous phase, which allowed the rejection of non-basic impurities in the organic phase. Then the aqueous phase was pH adjusted to ∼10, and the product was extracted with an organic solvent.

(14) DeBaillie, A. C.; Jasper, P. J.; Li, S.; McCulley, M. J.; Vaidyaraman, S.; Zhang, Z. Optimization of an Aminothiazine Ring Formation: Integrating Modeling with Experiments to Maximize Yield by Minimizing Impurity Formation. *Org. Process Res. Dev.* **2015**, *19*, 1244−1256.

(15) Though those impurities were longer present as more robust processes were implemented in subsequent campaigns.

(16) Li, B.; Weisenburger, G. A.; McWilliams, J. C. Practical Considerations and Examples in Adapting Amidations to Continuous Flow Processing in Early Development. *Org. Process Res. Dev.* **2020**, *24*, 2311−2318.

https://doi.org/10.1021/acs.oprd.1c00126
Org. Process Res. Dev. 2021, 25, 1440−1453